

# Effect of Difunctional Acids on the Physicochemical, Thermal, and Mechanical Properties of Polyester Polyol-Based Polyurethane Coatings

Wen Xu,<sup>1</sup> Lipan Zhou,<sup>2</sup> Weifu Sun,<sup>3</sup> Junrui Zhang,<sup>2</sup> Weiping Tu<sup>2</sup>

<sup>1</sup>College of Materials and Mineral Resources, Xi'an University of Architecture and Technology, Xi'an, People's Republic of China, 710055

<sup>2</sup>School of Chemistry and Chemical Engineering, South China University of Technology, Guangzhou, People's Republic of China, 510640

<sup>3</sup>School of Materials Science and Engineering, The University of New South Wales, Sydney, 2052, Australia  
Corresponding to: W. P. Tu (E-mail: cewptu@scut.edu.cn) and W. F. Sun (E-mail: weifu.sun518@gmail.com)

**ABSTRACT:** Polyester polyol (PP)-based polyurethanes (PUs) consisting of two difunctional acids [1,4-cyclohexanedicarboxylic acid (CHDA) and 1,6-adipic acid (AA)] and also two diols [1,4-cyclohexanedimethanol (CHDM) and 1,6-hexanediol (HDO)] were synthesized by a two-step procedure with a variable feed ratio of CHDA to AA but fixed ratio of CHDM and HDO. The prepared PPs and/or PUs were characterized by Fourier transform infrared spectroscopy, X-ray diffraction spectroscopy, and atomic force microscopy. The effects of difunctional acids on the thermal, mechanical, and dynamic mechanical thermal properties of PPs or PU films were investigated by thermogravimetry analysis, differential thermogravimetry and dynamic mechanical thermal analysis. The results show that PP exhibits a lowest viscosity with the mole fraction of CHDA and AA at 3 : 7 whereas it delivers a lowest melting point with the mole fraction at 9 : 1. After PPs being cross-linked by isocyanate trimers, the impact resistance, shear strength and glass transition temperature increase the mixed-acid formulations with increasing the content of CHDA. In detail, the resultant PU almost simultaneously exhibits the best mechanical and thermal properties when the mole fraction of CHDA and AA is kept constant at 9 : 1, thus giving rise to a high glass transition temperature of 56.4°C and an onset decomposition temperature of 350°C, and also delivering a balanced toughness and hardness with an impact resistance of 100 J/g and storage modulus as high as 10<sup>9</sup> Pa. This path for synthesis of PP-based PU provides a design tool for high performance polymer coatings. © 2014 Wiley Periodicals, Inc. *J. Appl. Polym. Sci.* 2015, 132, 41246.

**KEYWORDS:** coatings; mechanical properties; polyesters; polyurethanes; thermal properties

Received 9 March 2014; accepted 2 July 2014

DOI: 10.1002/app.41246

## INTRODUCTION

Polyurethane (PU) resins are generally prepared via a polyaddition reaction between a polyester polyol (PP) and an isocyanate.<sup>1–3</sup> The PU molecular structure and properties vary over a wide range of stiffness or flexibility, and variously formulated PUs are widely used in the packaging, coating industry, and nanocomposites<sup>4</sup> due to their excellent tensile strength, shear strength, dent resistance, hardness, and chemical resistance.<sup>5,6</sup> Hydroxyl-terminated polyesters, as one of the most common polyols, can be cross-linked by isocyanate groups. The macroscopic properties of the resulting compounds are critically dependent on the chemical composition and molecular weight distribution of the incorporated soft blocks (i.e., polyols). The polyesters that are composed by monomers with symmetrical

carbon atoms have high degree of crystallization, thus giving rise to the reduced mobility of their hard blocks. But the symmetrical carbon atoms introduced by the monomers in polyester backbone could improve the geometric fit of —NH to C=O, especially for PU in which both soft and hard blocks contain the same monomers.<sup>7</sup> Stanford et al. reported that the increasing functionality of soft blocks significantly increases the strength of PU, and decreases the overall degree of phase separations because of the increased compatibility of domain boundary.<sup>8</sup> Ramanuj Narayan et al. synthesized a series of PUs based on diols including neopentyl glycol, 1,4-cyclohexanedimethanol (CHDM) and 1,3-propane diol, respectively, revealing that the 1,4-CHDM-based PU coatings display higher solids content and better mechanical properties than the other two

diols.<sup>9</sup> It is also known that the viscosity of polyesters depends on the structure of diols:<sup>10</sup> the PPs synthesized with 1,6-hexanediol (HDO) have the lowest viscosity, followed by intermediate viscosity when synthesized with 2-butyl-2-ethyl-1,3-propanediol (BEPD) and hydroxypivalyl hydroxypivalate (HPPV), and highest viscosity when synthesized with the diols of CHDM and neopentyl glycol (NPG). Ni et al.<sup>11</sup> reported that the polyesters based on cycloaliphatic diacids have better solubility than the polyesters based on the aromatic or linear aliphatic diacids, but the cycloaliphatic diacids based PU coatings had intermediate mechanical and viscoelastic properties compared with PU based on aromatic and linear aliphatic diacids. Haseebuddin et al.<sup>12</sup> prepared PU by PPs synthesized with 1,6-adipic acid (AA) and isophthalic acid, showing that the synthesized PU has better mechanical properties with the mole ratio of AA and isophthalic acid at 1 : 1. This can be understood in terms of the chemical composition: the isophthalic acid improves the rigidity while AA enhances the flexibility of PU coatings. Besides, Singh et al.<sup>13</sup> discovered that the yellow color developed in the PU clear coatings is attributed to the structural transformation arisen from the visible spectrum absorbed by the aromatic benzene ring with conjugated  $\pi$ -electrons. Therefore, benzene ring should be removed from PU structure in order to enhance its weathering resistance.

It is reported that isocyanates, such as cycloaliphatic and aromatic isocyanate, acting as hard blocks of PU coatings, can enhance outdoor durability of high-solids, 1,4-cyclohexanedicarboxylic acid (1,4-CHDA) or 1,3-cyclohexanedicarboxylic acid (1,3-CHDA)-based two-component pigmented PU coatings.<sup>10,14–16</sup> Thermal properties of PU are significantly affected by the structure of isocyanate.<sup>17–20</sup> For instance, the PU prepared by the cycloaliphatic diacids has higher glass transition temperature than those prepared by linear aliphatic diacids. Moreover, aromatic isocyanates can endow polyesters with the most excellent mechanical properties than cycloaliphatic and linear aliphatic diacids.<sup>17–20</sup> Although aromatic ring can absorb ultraviolet (UV) light and hence improve the weather resistance property of isocyanate-based PU resins, the phenyl-ring can also absorb UV-light and limits their photo-oxidative stability.<sup>11,18,19</sup> Isocyanate trimers, such as isophorone diisocyanate (IPDI) and hexamethylene diisocyanate (HDI) trimers, were used because of their wide applications in industry. Gite et al. prepared PU cast films with excellent chemical resistance using IPDI trimer.<sup>21</sup> In the synthetic process, the PU-based samples can be properly cross-linked by the trimers without further adding cross-linking agent.

To the best of our knowledge, a variety of PUs has been designed in virtue of different formulas and some progress has been made thus far. However, high performance PUs still remain intensively pursued,<sup>22,23</sup> and little research has been done to simultaneously achieve desirable balanced thermal and mechanical properties. In order to achieve a PU with balanced thermal and mechanical properties, herein, the cycloaliphatic acid (i.e., 1,4-CHDA and 1,6-AA) and diols (i.e., 1,4 CHDM, 1,6-HDO) were used to prepare PPs, followed by being cross-linked by the isocyanate trimers (i.e., IPDI and HDI trimers).

The synthesized PU film were characterized by Fourier transform infrared spectroscopy (FTIR), X-ray diffraction (XRD) spectroscopy, and atomic force microscopy (AFM) and the mechanical and thermal properties such as viscosity, crystallization, impact resistance, shear strength, storage modulus, heat degradation, and glass transition temperature, will be explored using thermogravimetry analysis (TGA), differential thermogravimetry (DTG), and dynamic mechanical thermal analysis (DMTA).

## EXPERIMENTAL

### Materials

All analytical purity chemical reagents, that is, the difunctional acid 1,4-CHDA, 1,6-AA, 1,4-CHDM, 1,6-HDO, trimethylolpropane (TMP), the defoaming agent (TEGO Airex 932), the leveling agent (TEGO Glide 410), and the catalyst dibutyltin dilaurate (DBTDL) were purchased from Shanghai EHSY Corporation, China. The cross-linkers IPDI and HDI were provided by Bayer Corporation (Germany). Butyl-acetate from FUYU Chemical, China was used.

### Preparation of PPs

PPs were synthesized in a four-necked round-bottom flask equipped with mechanical stirrer, nitrogen purge, and a modified Dean&Stark condenser. The reaction was carried out under nitrogen purge at 210°C and the 0.0013 wt % BC-98 esterification catalyst was used. The conversion of PPs was monitored by measuring the acid value at different times until the acid value became  $\leq 1.5$  mg KOH/g. The acid value and hydroxyl values of polyesters were measured according to the ASTM standards D 1639-89 and D 4274-94, respectively. It should be noted that in this work, the acid value was measured about 9 hours since the chemical reaction commenced. Then, the solvent was exported every half an hour, followed by measuring the acid value. Besides, there is no significant effect of the CHDA/AA ratio on the time that the reaction was completed.

### Preparation of PU Films

The PPs were diluted in butyl-acetate and then mixed with the cross-linkers of IPDI and HDI trimer in a mass ratio of 2 : 1, the defoaming agent (TEGO Airex 932, 0.4 wt %), the leveling agent (TEGO Glide 410, 0.1 wt %), and the catalyst dibutyltin dilaurate (DBTDL, 0.01 wt %). The ratio of isocyanate group to hydroxyl group was kept constant at the mole ratio of 1.2 : 1.0. The mixture was put aside for a few minutes after it was well stirred. Then the mixture was divided into two parts: One of the films was cast on the aluminum panels which were ungreased with ethyl alcohol with thickness of 0.3 mm by a film applicator for general mechanical tests while the other part was cast on polyfluortetraethylene plates with thicknesses of 1.0–12.5 mm for shear strength tests. The films were cured at 80°C for 2 h, and the cured films were then stored for 5 days under ambient atmospheric conditions for future tests.

### Characterizations

The molecular weights were controlled by hydroxyl number, which was determined by titration. The number average molecular weight ( $M_n$ ) and weight average molecular weight ( $M_w$ ) of PPs were determined by gel permeation chromatography (GPC)

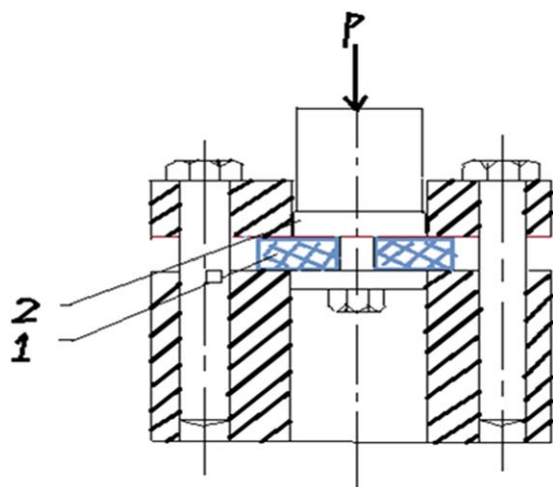
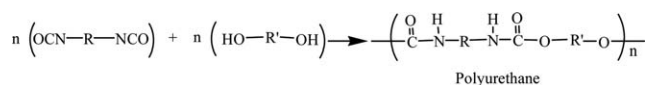


**Figure 1.** The puncher with sample applied with pressure. Numbers 1 and 2 represent the sample plate and the puncher, respectively. [Color figure can be viewed in the online issue, which is available at [wileyonlinelibrary.com](http://wileyonlinelibrary.com).]

by diluting polyesters in tetrahydrofuran (THF) with the mass fraction being 3%–5%, which was applied as mobile phase and delivered at a rate of 1.0 mL/min, then the polydispersity index (PDI) is calculated by  $PDI = M_w/M_n$ . The calibration curve was generated by using a narrow molecular weight distribution of polystyrene. The melting points were measured on a differential scanning calorimeter (DSC) with a heating rate of 10 K/min. The viscosity was measured on a rotation viscometer DV-2 PRO+ at room temperature.

The impact resistance (ASTM D2794) and resistance to cracking (3.2 mm in mandrel size) and elongation (ASTM D522) were measured according to ASTM standards. Abrasion resistance was determined according to national standard of China GB1768-79.<sup>24</sup> The coated round glass boards were rubbed for 200 cycles by 120# rubber abrasive wheel under 1 kg load. The abrasion resistance was evaluated from the average weight loss of three parallel tests. The chemical structures of PUs were characterized by attenuated total reflectance (ATR) sampling technique and FTIR using Bruker Vector 33 from Germany. The Bruker D8 ADVANCE was used for XRD with a wavelength of 0.15418 nm and  $2\theta$  scanning in the range of  $4^\circ$ – $50^\circ$ . The thermal analyzer NETZSCH STA 449C was employed and the sample was heated from room temperature to  $600^\circ\text{C}$  at a heating



**Scheme 1.** The reaction route of the synthesis of polyurethane

rate of 10 K/min in nitrogen atmosphere at 20 mL/min. The viscoelastic properties of the cross-linked films were obtained with DMTA using NETZSCH DMA 242 (United States) with a frequency of 10 Hz and a heating rate of  $3^\circ\text{C}/\text{min}$  over the range of  $-70^\circ\text{C}$ – $150^\circ\text{C}$ . The morphology was taken by AFM on SPA400 with an SPI3800N controller (Seiko Instruments Industry, Co., Ltd) at room temperature. The crosslink density ( $\nu_e$ ), that is, the molar number of elastically effective network chains per cubic centimeter of a sample, was calculated from the formula:  $\nu_e = \dot{E}/3RT$ , ( $T \gg T_g$ , at least  $50^\circ\text{C}$  greater than  $T_g$ ) where  $\dot{E}$  is the tensile storage modulus at the corresponding temperature  $T$  (here  $120^\circ\text{C}$  was used),  $R$  is the gas constant of 8.31 J/(mol K) and  $T$  is Kelvin temperature.<sup>16,25</sup> The shear strength of PU was tested by a punching tool. A circular puncher as shown in Figure 1 was used and the force was imposed on the samples by a universal material tester to cause shear deformation or damage to measure the shear strength. The samples should be smooth and flat, in squared (50 mm in length) or circled shape (50 mm in diameter) with no mechanical damage or impurities, while the thickness being homogeneous at 0.5–3.0 mm. There is a punch hole (11 mm diameter) in the center of the samples. The speed of test was 1 mm/min. More than five samples were tested for each film. The results were calculated in arithmetic mean with three significant figures. The shear strength ( $\sigma_t$ ) was calculated by using the following equation:

$$\sigma_t = \frac{P}{\pi Dh} \quad (1)$$

where  $P$  is the shear load (N) at which shear deformation started as shown in Scheme 1,  $\pi$  is the circumference ratio,  $D$  is the diameter of the puncher (mm), and  $h$  is the thickness of sample (mm).

## RESULTS AND DISCUSSION

A two-step procedure was adopted for the preparation of PP-based PUs. The first step involved the synthesis of PPs consisting of 1,4-CHDA, 1,6-AA, 1,4-CHDM, and 1,6-HDO. The formulations of all polyesters used are listed in Table I. The mole ratio of diol to difunctional acid is kept fixed at 1.28 : 1 while

**Table I.** The Formulation of Different PPs (Mol)

Polyester polyols	HDO	CHDM	TMP	AA	CHDA	CHDA/AA
PP-1	0.48	0.16	0.06	0.50	0.00	0 : 1
PP-2	0.48	0.16	0.06	0.45	0.05	1 : 9
PP-3	0.48	0.16	0.06	0.35	0.15	3 : 7
PP-4	0.48	0.16	0.06	0.25	0.25	5 : 5
PP-5	0.48	0.16	0.06	0.15	0.35	7 : 3
PP-6	0.48	0.16	0.06	0.05	0.45	9 : 1
PP-7	0.48	0.16	0.06	0.00	0.50	1 : 0

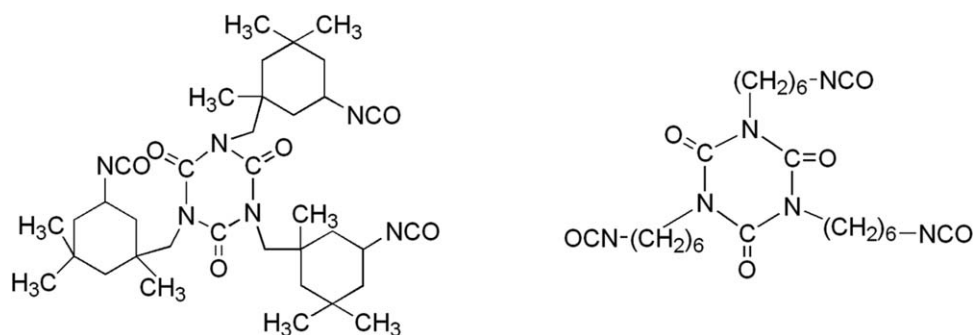


**Figure 2.** The chemical structures of isophorone diisocyanate (IPDI, left) and hexamethylene diisocyanate (HDI, right) trimer.

the mole ratio of 1,6-HDO to 1,4-CHDM is kept constant at 3 : 1 and also the amount of diols are constant relative to those of difunctional acids, thus enabling to achieve the identical average molecular weight. In contrast, the mole ratio of 1,6-AA to 1,4-CHDA is varied to synthesize a series of PPs with different chemical compositions. PP-1 has 1,6-AA only while PP-7 contains 1,4-CHDA only. Whereas PP-2, PP-3, PP-4, PP-5, and PP-6 are made up of 1,6-AA and 1,4-CHDA at different mole ratios but containing the identical amount of trimethylolpropane (TMP). The second step is the cross-linking of PPs using isocyanate trimers including IPDI and HDI trimers and their chemical structures are shown in Figure 2.

#### FTIR Analysis

The FTIR spectra of three samples PP-1, PP-6, and PP-7 are shown in Figure 3. The absorption bands at 2938 and 2867  $\text{cm}^{-1}$  are related to C—H stretching vibrations for alkane groups. The existence of these groups was confirmed by the presence of bands at 1457 and 1371  $\text{cm}^{-1}$ , which corresponds to a C—H bending vibration in the molecules. The peak at 1730  $\text{cm}^{-1}$  is the characteristic frequency for C=O group while the band at 1175  $\text{cm}^{-1}$  is related to C—O vibration of the ether group from PP samples. The spectra also illustrate the feature frequency for O—H stretching vibration at 3540  $\text{cm}^{-1}$ . From the above FTIR spectra characterization, it is found that the hydroxyl-terminated PPs were synthesized.

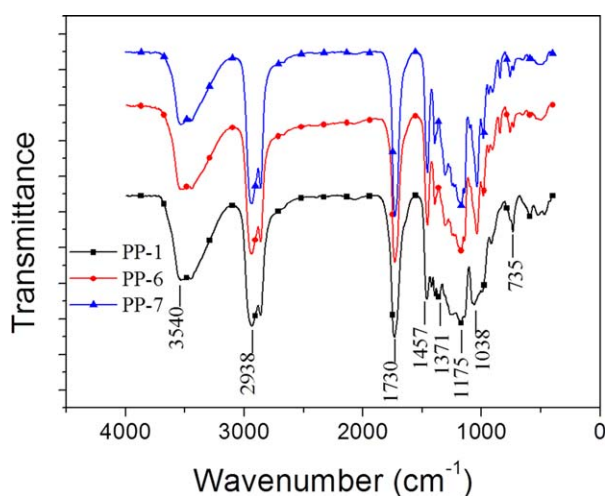


**Figure 3.** The FTIR spectra of PPs. [Color figure can be viewed in the online issue, which is available at [wileyonlinelibrary.com](http://wileyonlinelibrary.com).]

The content of 1,4-CHDA increases while the amount of AA decreases from samples PU-1 to PU-7. The films made from samples PU-1 to PU-7 were characterized to probe layers of adsorbed/deposited species at a solid/liquid interface by ATR sampling technique and FTIR.<sup>26,27</sup> The crosslinking chemical reactions can be represent by the following scheme,

As shown in Figure 4, multiple absorption bands reflecting complex properties of hydrogen bonding in the PU films are observed. The spectra characterized by absorption bands positioned at approximately 1727  $\text{cm}^{-1}$  and approximately 1680  $\text{cm}^{-1}$  is ascribed to the carboxyl absorption band of PU, that is, —COOR', and the absorption band at approximately 3365  $\text{cm}^{-1}$  is attributed to the N—H group. Two weak shoulders at 2930 and 2840  $\text{cm}^{-1}$  are assigned to the groups of methyl or methylene from the carbon chain. But there is no adsorption band in the range of 2275–2250  $\text{cm}^{-1}$ , which is pertinent to the N=C=O group, indicating that the PU is almost completely cured and cross-linked.

#### Properties of Polyesters

The initially synthesized PPs were characterized and the physical quantities including the acid value, hydroxyl value, the number average molecular weight ( $M_n$ ), viscosity, and melting point, were summarized in Table II. It is clear that the acid value, number average molecular weight ( $M_n$ ) of about 3000 g/mol

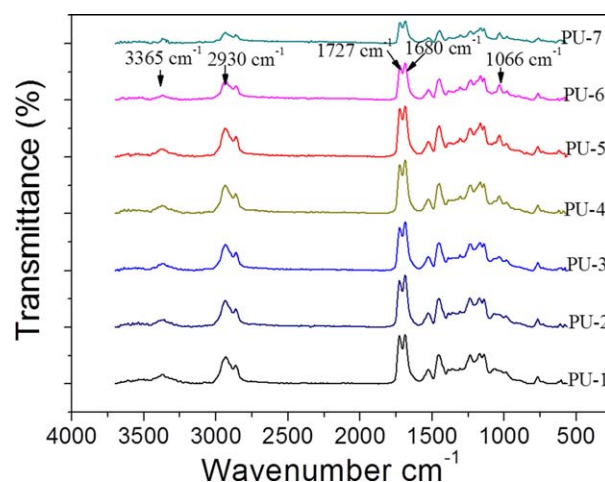


**Figure 4.** The ATR FTIR spectra of PU films. [Color figure can be viewed in the online issue, which is available at [wileyonlinelibrary.com](http://wileyonlinelibrary.com).]

**Table II.** The Properties of Polyester Polyols

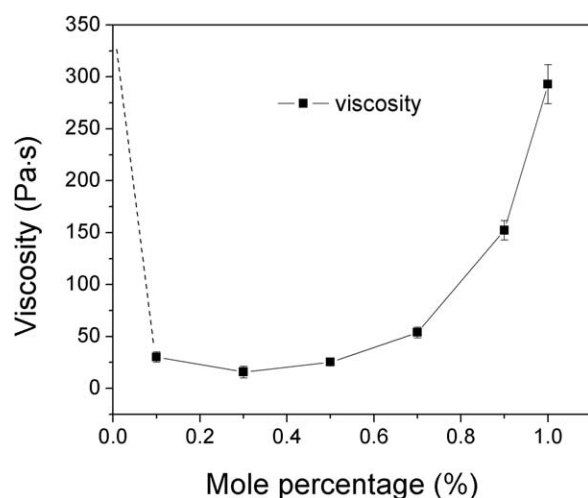
PP	Acid-value (mg KOH/g)	Hydroxyl-value (mg KOH/g)	$M_n$ (g/mol)	PDI	Viscosity (Pa s)	$T_m$ (°C)
PP-1	1.4 ± 0.21	102.3 ± 5.5	2980 ± 35	1.22 ± 0.25	-	33.9 ± 2.7
PP-2	1.5 ± 0.18	106.8 ± 3.6	3284 ± 43	1.30 ± 0.19	30.2 ± 4.9	14.4 ± 1.5
PP-3	1.3 ± 0.22	105.7 ± 4.5	2999 ± 31	1.23 ± 0.26	15.7 ± 5.7	9.5 ± 0.9
PP-4	1.1 ± 0.25	98.3 ± 3.7	3093 ± 27	1.26 ± 0.26	25.3 ± 3.3	5.3 ± 0.5
PP-5	1.5 ± 0.21	92.6 ± 4.3	3036 ± 31	1.24 ± 0.21	53.8 ± 5.1	1.9 ± 0.4
PP-6	1.5 ± 0.17	86.1 ± 3.1	3127 ± 23	1.27 ± 0.18	152.2 ± 9.4	0.7 ± 0.1
PP-7	1.4 ± 0.18	93.8 ± 2.9	3066 ± 28	1.25 ± 0.22	292.9 ± 18.7	4.3 ± 0.6

and the PDI as determined by  $PDI = M_w/M_n$  are similar among these seven samples studied, but the sample PP-6 with the mole ratio of 1,4-CHDA and 1,6-AA at 9 : 1 has the lowest hydroxyl number of 86.1 mg KOH/g and also the smallest melting point of 0.7°C only.

As viscosity is one of the important parameters for polymers, emphasis is given to the discussion of this physical quantity herein, which was characterized by rotation viscometer at room temperature. Figure 5 shows the viscosity of PPs obtained at different mole ratios of AA to 1,4-CHDA acid. The viscosity of PPs first decreases rapidly at the very beginning, and then a minimum viscosity of 15.7 Pa s is observed when the mole percentage of 1,4-CHDA is about 30%. After that, the viscosity monotonously increases with increasing the mole percentage of 1,4-CHDA. The viscosities of molten linear polymers can be correlated to the molecular weights and the relationship reported by Flory is given by<sup>28</sup>

$$\log \eta = A + CZ_w^{1/2} \quad (2)$$

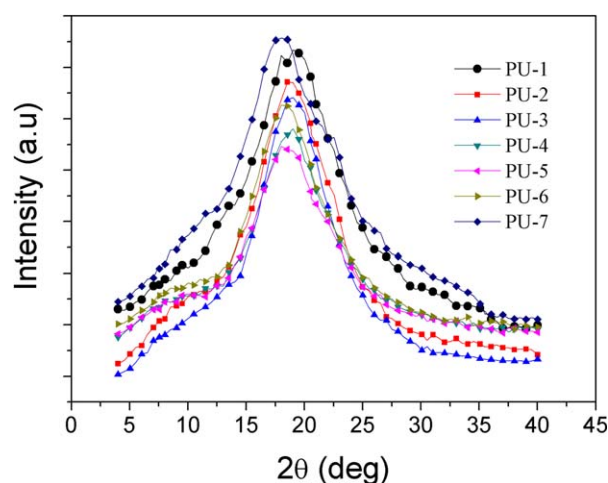
where  $\eta$  is the viscosity,  $Z_w$  is the weight average chain length, and  $A$  and  $C$  are constants. Normally, the viscosity of polyesters should decrease with decreasing the mole percentage of AA (i.e.,

**Figure 5.** The viscosity of PPs-based on the AA and 1,4-CHDA as a function of the mole fraction of 1,4-CHDA.

the increasing content of 1,4-CHDA) of the linear structure. However, because of the polycondensation of 1,4-CHDA,<sup>29</sup> the viscosity of PPs reaches a minimum with the mole percentage of 1,4-CHDA and 1,6-AA being 30% and 70%, respectively, followed by increasing gradually with the increasing content of 1,4-CHDA. Thus, the content of AA dominates the viscosity trend of PPs at the beginning while 1,4-CHDA gradually becomes dominant with the increase in the content of 1,4-CHDA. After the formulation optimization, the lowest viscosity of 15.7 Pa s can be achieved at the mole percentage of 1,4-CHDA at about 30%. This value is comparable to the similar formulation of polyesters reported elsewhere, around 10 Pa s.<sup>11,16,30</sup> The differences, on one hand, can be ascribed to the different diols that were used during synthesis; on the other hand, such discrepancy is, to a large degree, within experimental error.

#### XRD Pattern of PUs

Figure 6 shows the XRD pattern of the samples PU-1 to PU-7. It reveals that there is a  $2\theta$  diffraction peak at approximately 20°, which is in reasonable agreement with the reported value of PU elsewhere.<sup>16,31,32</sup> The intensity of this peak gradually decreases from samples PU-1 to PU-5, followed by a reverse increase from PU-6 to PU-7. In other words, samples PU-1 and PU-7 have the strongest diffraction intensity. This can be

**Figure 6.** The XRD patterns of PUs. [Color figure can be viewed in the online issue, which is available at [wileyonlinelibrary.com](http://wileyonlinelibrary.com).]

**Table III.** Mechanical Properties of PUs

PU	$T_g$ (°C)	Impact resistance (J/g)	Weight loss (g)	Cracking resistance	Shear strength (MPa/s)
PU-1	29.4 ± 1.1	54.9 ± 2.6	0.026 ± 0.002	Pass	23.2 ± 2.1
PU-2	42.8 ± 1.5	70.1 ± 3.5	0.019 ± 0.001	Pass	33.1 ± 2.0
PU-3	43.1 ± 2.5	75.2 ± 4.5	0.017 ± 0.002	Pass	36.7 ± 2.0
PU-4	49.8 ± 2.0	79.8 ± 5.6	0.014 ± 0.001	Pass	50.3 ± 4.2
PU-5	50.5 ± 1.3	85.3 ± 4.7	0.013 ± 0.002	Pass	51.5 ± 2.5
PU-6	56.4 ± 2.0	100.3 ± 6.1	0.010 ± 0.002	Pass	54.3 ± 2.8
PU-7	50.5 ± 1.9	90.2 ± 5.4	0.011 ± 0.001	Fail	57.7 ± 3.6

interpreted in terms of molecular structure, especially, the soft segments of the components. The soft segments of PU-1 consist of AA only with the most regular structure (linear), while soft segments of PU-7 contain CHDA only, which becomes more rigid than AA. For these two limiting cases, the non-polar property of soft segments of AA or CHDA leads to poor segment compatibility but better separation of the hard-soft segments, which in turn facilitates the possible growth of microcrystalline structure, therefore sample PU-1 and PU-7 display relatively stronger intensity of diffraction peak. As for the intermediate samples, PU-2 to PU-6 are made from the mixture of AA and CHDA, in which the polarity of soft segments improves the segment compatibility, consequently it gives rise to the decreased structural regularity and crystallization.<sup>33</sup>

### Mechanical Properties

The mechanical properties of PUs are summarized in Table III. Both the impact resistance and abrasion resistance gradually increase from sample PU-1 to PU-6, and reaches a maximum value of PU-6 that is prepared at the mole percentage of 1,4-CHDA and AA is 90% and 10%, respectively. Notably, the impact resistance of sample PU-7 containing only 1,4-CHDA is not the largest one, which also fails the test of resistance to cracking, although it delivers the highest shear strength. The results also show that the prepared PU films exhibit good abrasion resistance and most of them demonstrate a weight loss less

than 0.02 g, especially the PU-6 presents the best abrasion resistance with the minimum weight loss.

These phenomena can be explained by the structural changes of the PU. The physical and mechanical properties of a PU depend primarily on whether or not there is microphase separation and its extent.<sup>34</sup> Generally, the higher the rigidity of chains in PU is and the softer the flexible chains are, the more easily microphase separation will take place, and the better the physical and mechanical properties will be. Adding a certain amount of low hardness, high-resilience AA can increase the softness of the flexible chain. This is beneficial to microphase separation. However, excessive AA will undermine the continuity of the matrices, affecting the microphase separation, thus decreasing the mechanical properties. Sample PU-7 made from 1,4-CHDA only does not have good flexibility due to the lack of AA because it is believed that 1,6-AA can improve the flexibility. Furthermore, the shear strength  $\sigma_s$  always increases from sample PU-1 to PU-7. This can be ascribed to the fact that as the content of 1,4-CHDA increases from PU-1 to PU-7, the 1,4-CHDA can provide hardness to the synthesized PU resins while AA can endow flexibility to the PU.<sup>35</sup> In this work, the incorporation of 1,6-AA and 1,4-CHDA into PU is designed to achieve a balanced mechanical property between hardness and toughness (i.e., flexibility). While 1,6-AA can improve the flexibility, but it has an adverse effect on the outdoor durability because of the

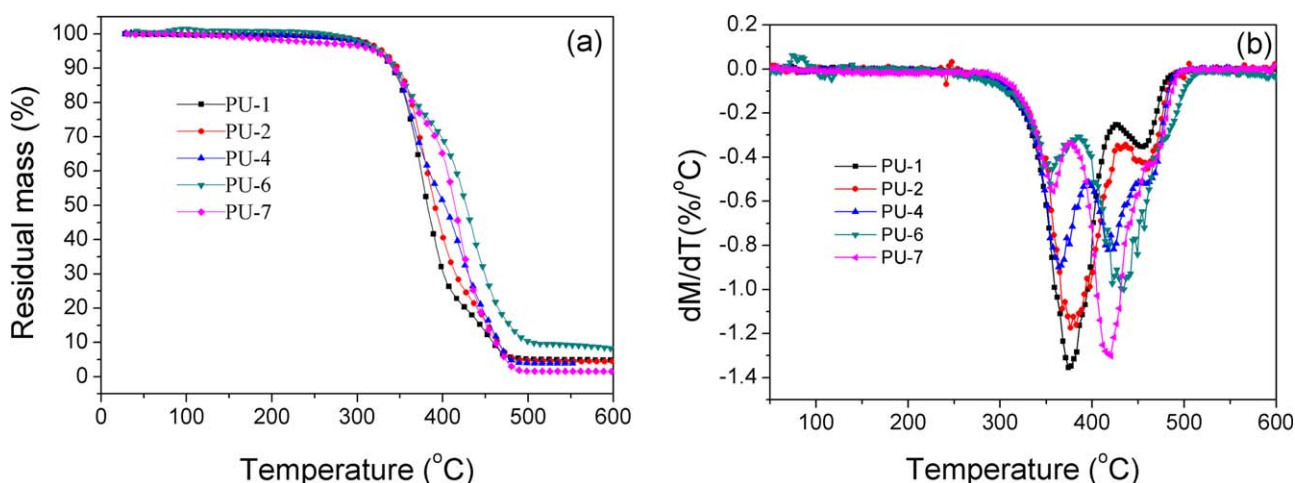


**Figure 7.** The TG (a) and DTG (b) curves of PU samples. [Color figure can be viewed in the online issue, which is available at [wileyonlinelibrary.com](http://wileyonlinelibrary.com).]

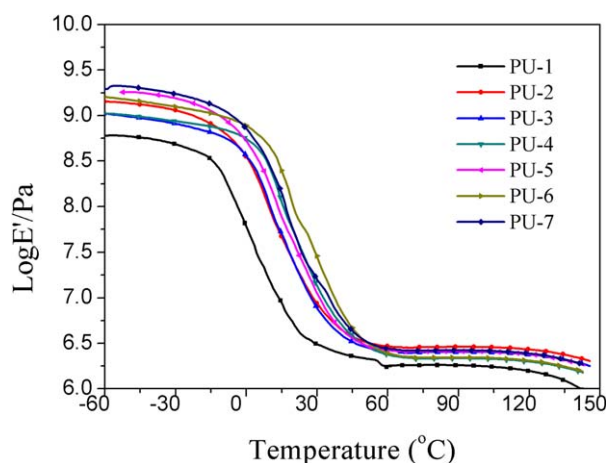


**Figure 8.** Dependence of  $\text{Log} E'$  on temperature for a variety of PU films. [Color figure can be viewed in the online issue, which is available at [wileyonlinelibrary.com](http://wileyonlinelibrary.com).]

lack of hardness, thus 1,4-CHDA was introduced to provide hardness and overcome this shortcoming. Likewise, Awasthi et al.<sup>36</sup> employed AA/isophthalic acid (IPA) to achieve a hardness/flexibility balance in coating films. Generally speaking, the sample PU-6 has the better mechanical property than other samples. In a short summary, the sample PU-6 delivers a comprehensive and best mechanical property in terms of impact resistance, shear strength and also resistance to cracking. Furthermore, as will be discussed from Figure 7, it also exhibits the highest storage modulus with the mole ratio of 1,4-CHDA to 1,6-AA at 9 : 1.

### Thermal Analysis

The thermal degradation and stability of PUs were studied by TG and DTG analysis. Figure 7 shows the TG and DTG curves of PUs decomposed in nitrogen atmosphere at a heating rate of 10°C/min. As observed from Figure 7, the decomposition of

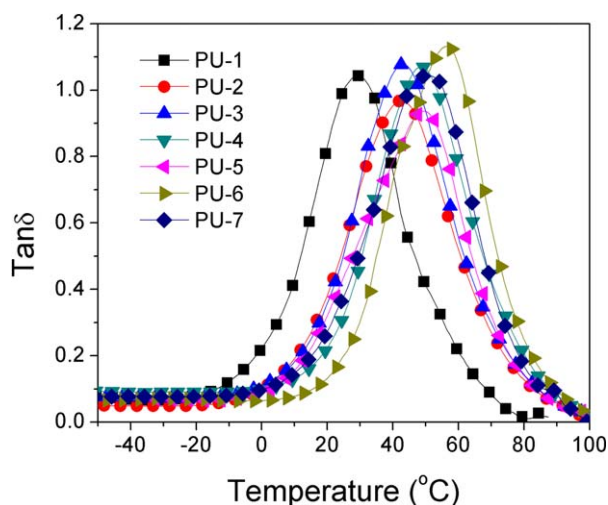


**Figure 9.** Dependence of  $\tan \delta$  of PU films on temperature. [Color figure can be viewed in the online issue, which is available at [wileyonlinelibrary.com](http://wileyonlinelibrary.com).]

PUs begins at approximately 330°C and ends at approximately 490°C [Figure 7(b)], and about 90 wt % of PUs was lost during the decomposition process [Figure 7(a)]. Especially, the decomposition temperature of PU-1 is the lowest one while PU-6 has the highest decomposition temperature. A Gauss type deconvolution of DTG curve was used for a better assessment of the thermal degradation process [Figure 7(b)]. Carbon dioxide was found to be the most abundant product during the first step of degradation (350°C–380°C) in nitrogen atmosphere. At the second degradation stage (420°C–490°C), a much more complex mixture originated from the degradation of polyol-segment was identified.<sup>37</sup> From the viewpoint of molecular structure, the thermal degradation and stability of PUs can be correlated to the structures of the hard and soft segments.<sup>38</sup> By increasing the content of CHDA from sample PU-1 to PU-7, the degrading rate at first step gradually decreases while the degrading rate at the second stage increases from samples PU-1 to PU-7. This indicates that the scission of linear carbon chain of AA takes place first at 350°C–380°C and the degradation of hexatomic ring of CHDA occurs subsequently at 420°C–490°C.

### Dynamic Mechanical Thermal Properties of PUs

One of the advantages of DMTA is that it can provide sensitive measurement of the physical changes occurring to polymers over a wide range of temperatures and frequencies. The representative logarithm storage modulus ( $\text{log} E'$ ) and loss angle  $\tan \delta$  peaks for PUs are plotted against temperature as shown in Figures 8 and 9, respectively. It can be observed from Figure 8 that the storage moduli of PUs decrease sharply in the temperature range from 15°C to 60°C, and such decrease of the modulus indicates a stiffness loss of PUs.<sup>39</sup> Then, the curves gradually level off and do not change much after 80°C. Generally, the modulus of hard materials<sup>40</sup> and elastic materials<sup>41</sup> is 1–10 GPa and 1 MPa, respectively. Strikingly, the modulus of most of the PUs was estimated to be about 1–2 GPa below 20°C from Figure 8. Such high modulus demonstrates the excellent mechanical properties of the synthesized PU resins. Interestingly, the sample PU-6 displays the highest modulus among these samples with the modulus being about approximately 2 GPa in the temperature range of approximately 0°C–38°C and the highest loss angle  $\tan \delta$  peak at approximately 56.4°C (Figure 9). The cross-link density ( $\nu_e$ ), that is, the molar number of elastically effective network chains per cubic centimeter of a sample, was roughly estimated calculated and the results were shown in Table IV. In preparing the PU films, IPDI and HDI trimer could act as physical or chemical crosslinking points. The cross-linker can typically involve the chemical reactions, then acting as chemical crosslinking, but also due to the intermolecular forces, such as van der Waals attraction force,<sup>42,43</sup> hydrogen bonds, the physical crosslinking coexists.

The large difference in modulus between below and above the transition temperature and a sharp glass transition temperature ( $T_g$ ) are the most important parameters for shape-formation of materials.<sup>44</sup> The glass transition temperature  $T_g$  can be determined by the point where  $\tan \delta$  reaches the maximum from Figure 9. It is clear that the  $\tan \delta$  firstly increases sharply to a maximum, followed by a drastic decrease. The estimated  $T_g$  of PU samples are listed in Table III. This phenomenon can be

**Table IV.** DMTA Results and Crosslink Density of the PU Films

PU	PU-1	PU-2	PU-3	PU-4	PU-5	PU-6	PU-7
$T_g$ (°C)	29.4	42.8	43.1	49.8	50.5	56.4	50.5
$E'$ (MPa)	1.571	2.698	2.377	1.987	2.033	2.433	2.392
$\nu_e$ (mol/m <sup>3</sup> )	160.38	275.40	242.69	202.85	207.57	248.41	244.14

understood from their structural changes of the PU films: with the increase of the ratio of CHDA to AA, the rigidity of the soft segment gradually increases and thus the glass transition temperature  $T_g$  increases. When the ratio reaches 9 : 1,  $T_g$  achieves a maximum value, meanwhile, the compatibility between the soft and hard segments becomes relatively poor, which favors the creation and propagation of microphase. Thus similar to the trend of impact resistance for PUs, the glass transition temperature gradually increases from 29.4°C to 56.4°C corresponding to the sample PU-1 to PU-6, but then decreases from PU-6 to PU-7 (Figure 9). Note that the observed  $T_g$  is in reasonable agreement with the reported value.<sup>45</sup> Moreover, as the width and shape of the  $\tan\delta$  are indicator of the heterogeneity of the ingredients used in the coatings formation,<sup>46</sup> as observed from Figure 9, the loss angle  $\tan\delta$  is almost symmetrical over the temperature, indicating that the coatings are fully cured and no additional curing occurred at the same time. Note that the  $\tan\delta$  curve of PU-6 almost has a hump around 40°C and this unsymmetrical shape may be ascribed to heterogeneity of the sample to some degree. In this field, there are some comprehensive and pioneering work done by Ni et al.,<sup>11,47</sup> in which difunctional diols, cycloaliphatic difunctional acids, adipic, azelaic, and isophthalic acids were all considered and different combinations were employed. The prepared PU coatings exhibit a glass transition temperature ranging from 45°C to 92°C measured by DMTA method and also a high storage modulus up to

1–2 GPa.<sup>11</sup> In contrast, this work focuses on the varied ratio of 1,4-CHDA and AA only and the effect of the varied ratio on the final properties of PU coatings was further explored in details. The resultant PU coatings (e.g., PU-6) exhibit comparable and balanced mechanical and thermal properties compared with the previous works.<sup>11</sup>

### Surface Morphology of PU

The morphology of sample PU-6 with the mole ratio of 1,4-CHDA and 1,6-AA at 9 : 1 was characterized by AFM and shown in Figure 10. Normally the hard region exhibits high modulus, thus appearing bright. The bright and convex regions represent hard phase while the relatively dark and concave regions represent soft phase (e.g., polyol). It can be observed that the soft segments (i.e., polyols) and hard segments (i.e., isocyanates) were well mixed and no obvious microphase separation was observed due to the good compatibility and also strong intermolecular forces such as van der Waals attraction force between them<sup>48,49</sup> (Figure 10). This is also consistent with the results from DMTA in Figure 9, in which only one  $\tan\delta$  peak was observed.

### CONCLUSIONS

In conclusion, we report the synthesis of a PU prepared by the initial reactions between two difunctional acids of 1,4-CHDA and 1,6-AA at varied mole ratios and two different diols (i.e.,

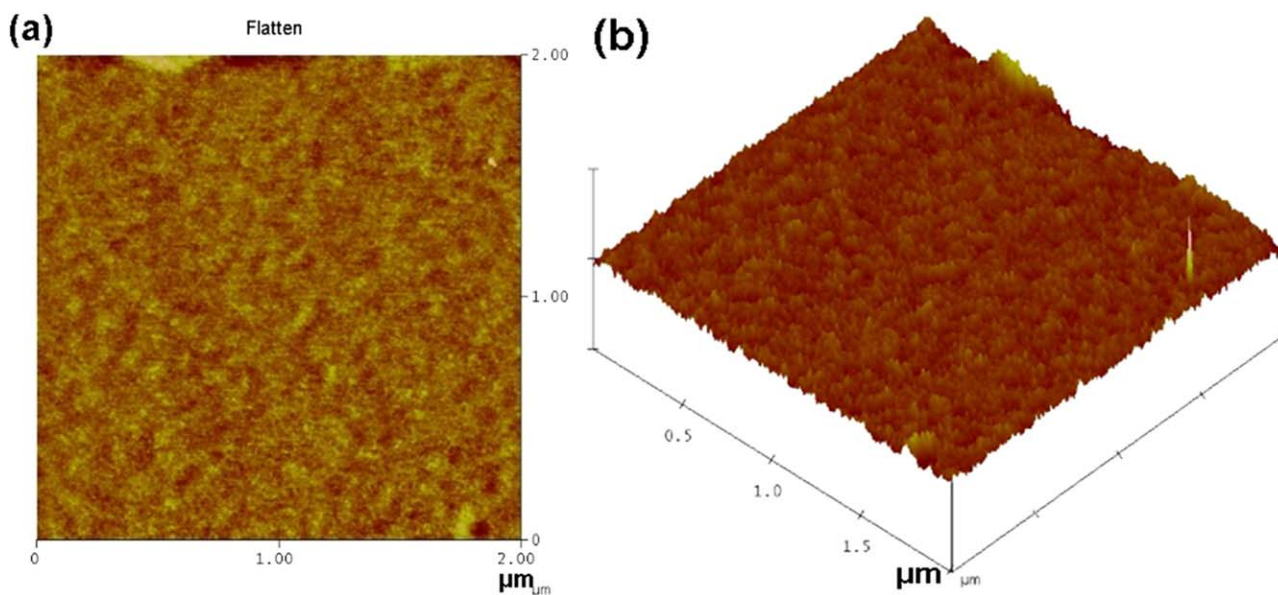


**Figure 10.** The phase image (a) and 3-dimensional (b) AFM images of PU of sample PU-6. [Color figure can be viewed in the online issue, which is available at [wileyonlinelibrary.com](http://wileyonlinelibrary.com).]



1,4-CHDM and 1,6-HDO) but at fixed mole ratio of 3 : 1 and also fixed ratio relative to the two difunctional acids, followed by cross-linking by IPDI and HDI trimers. The effect of the varied mole ratio of the two difunctional acids on the properties of the PPs was investigated first in terms of acid value, hydroxyl value, number average molecular weight, viscosity, and melting point. The results show that the acid number and number average molecular weight of PPs are similar; the minimum viscosity of the PPs is achieved at the mole percentage of 1,4-CHDA being 30%. Among the seven samples studied, the melting point of PP-6 with the mole percentage of 1,4-CHDA being 90% reaches a minimum value of 0.7°C. After PPs being cross-linked by the isocyanate trimers (i.e., IPDI and HDI trimer), the mechanical, thermal and dynamic mechanical properties of PUs are explored, revealing that the impact resistance, shear strength and glass transition temperature largely increase with increasing the content of CHDA. Surprisingly, it is unveiled that the sample PU-6 with the initial mole percentage of 1,4-CHDA and 1,6-AA being 90% and 10%, respectively, exhibits the best thermal and mechanical properties with  $T_g$  at 56.4°C and a onset decomposition temperature as high as 350°C, also delivers a balanced toughness and hardness with impact resistance up to 100 J/g and storage modulus as high as  $10^9$  Pa. The cycloaliphatic difunctional acids provide PUs with excellent mechanical and thermal properties and should hold promise in applications of transparent solar encapsulant film and other coating industry due to the low-cost, their high transmittance, mechanical and thermal properties, which can effectively protect solar cells from moisture, oxygen, weather, and scratch. And also those findings provide a design tool for the development of high-performance PUs.

## ACKNOWLEDGMENTS

The authors thank the support from the universities. This work is partly funded by National Key Laboratory Cultivation Base of Western China Construction Science and Technology jointly established by Shaanxi Province and Ministry of Education, and Talent Technology Fund of Xi'an University of Architecture and Technology (DB09065).

## REFERENCES

- Li, S. X.; Liu, Y. J. *Polyurethane Resin and Its Application*, 1st ed.; Chemical Industry Press: Beijing, **2008**.
- Saito, T.; Perkins, J. H.; Jackson, D. C.; Trammel, N. E.; Hunt, M. A.; Naskar, A. K. *RSC Adv.* **2013**, *3*, 21832.
- Knight, S. C.; Schaller, C. P.; Tolman, W. B.; Hillmyer, M. A. *RSC Adv.* **2013**, *3*, 20399.
- Huang, W. M.; Sun, W. F.; Chen, G. H.; Tan, L. *Adv. Eng. Mater.* **2014**, DOI:10.1002/adem.201400143.
- Sonnenschein, M. E.; Koonce, W. *Encyclopedia of Polymer Science and Technology*; John Wiley & Sons, Inc.: New York, **2002**.
- Tanzi, M. C.; Nicolais, L. *Wiley Encyclopedia of Composites*; John Wiley & Sons, Inc.: New York, **2011**.
- Chang, C. C.; Chen, K. S.; Yu, T. L.; Chen, Y. S.; Tsai, C. L.; Tseng, Y. H. *Polym. J.* **1999**, *31*, 1205.
- Stanford, J. L.; Still, R. H.; Wilkinson, A. N. *Polymer* **1995**, *36*, 3555.
- Narayan, R.; Raju, K. *Prog. Org. Coat.* **2002**, *45*, 59.
- Ni, H.; Daum, J. L.; Soucek, M. D.; Simonsick, W. J. *J. Coat. Technol. Res.* **2002**, *74*, 49.
- Ni, H.; Daum, J. L.; Thiltgen, P. R.; Soucek, M. D.; Simonsick, W. J.; Zhong, W.; Skaja, A. D. *Prog. Org. Coat.* **2002**, *74*, 49.
- Haseebuddin, S.; Padmavathi, T.; Raju, K.; Yaseen, M. *JOCCA-Surf. Coat. Int.* **1995**, *78*, 68.
- Singh, R. P.; Tomer, N. S.; Bhadrachari, S. V. *Polym. Degrad. Stabil.* **2001**, *73*, 443.
- Awasthi, S.; Agarwal, D. *J. Coat. Technol. Res.* **2009**, *6*, 329.
- Awasthi, S.; Agarwal, D. *J. Coat. Technol. Res.* **2007**, *4*, 67.
- Ni, H.; Skaja, A. D.; Sailer, R. A.; Soucek, M. D. *Macromol. Chem. Phys.* **1999**, *201*, 722.
- Oprea, S. *Adv. Polym. Tech.* **2009**, *28*, 165.
- Panwiriyyarat, W.; Tanrattanakul, V.; Pilard, J.-F.; Pasetto, P.; Khaokong, C. *J. Appl. Polym. Sci.* **2013**, *130*, 453.
- Corcuera, M. A.; Rueda, L.; Saralegui, A.; Martín, M. D.; Fernández-d'Arlas, B.; Mondragon, I.; Eceiza, A. *J. Appl. Polym. Sci.* **2011**, *122*, 3677.
- Xie, R.; Bhattacharjee, D.; Argyropoulos, J. *J. Appl. Polym. Sci.* **2009**, *113*, 839.
- Gite, V. V.; Mahulikar, P. P.; Hundiwale, D. G.; Kapadi, U. R. *J. Sci. Ind. Res.* **2004**, *63*, 348.
- Gu, X. Z.; Mather, P. T. *RSC Adv.* **2013**, *3*, 15783.
- Du, P. F.; Liu, X. X.; Zheng, Z.; Wang, X. L.; Joncheray, T.; Zhang, Y. F. *RSC Adv.* **2013**, *3*, 15475.
- Zhou, S. X.; Wu, L. M.; Sun, J.; Shen, W. D. *Prog. Org. Coat.* **2002**, *45*, 33.
- Zhang, Y.; Asif, A.; Shi, W. F. *Prog. Org. Coat.* **2011**, *71*, 295.
- Schwinte, P.; Voegel, J. C.; Picart, C.; Haikel, Y.; Schaaf, P.; Szalontai, B. *J. Phys. Chem. B* **2001**, *105*, 11906.
- Huanbutta, K.; Terada, K.; Sriamornsak, P.; Nunthanid, J. *Eur. J. Pharm. Biopharm.* **2013**, *83*, 315.
- Flory, P. J. *J. Am. Chem. Soc.* **1940**, *62*, 1057.
- Higashi, F.; Sugimori, S. *Macromol. Rapid Commun.* **2000**, *21*, 891.
- Soucek, M. D.; Ni, H. *J. Coat. Technol.* **2002**, *74*, 125.
- Hu, J. K.; Li, L.; Zhang, S. W.; Gong, L. B.; Gong, S. L. *J. Appl. Polym. Sci.* **2013**, *130*, 1611.
- Xu, J. W.; Shi, W. F.; Pang, W. M. *Polymer* **2006**, *47*, 457.
- Kozakiewicz, J. *Prog. Org. Coat.* **1996**, *27*, 123.
- Tan, J.; Ding, Y. M.; He, X. T.; Liu, Y.; An, Y.; Yang, W. M. *J. Appl. Polym. Sci.* **2008**, *110*, 1851.
- Marsh, S. J. *JCT CoatingsTech.* **2005**, *2*, 32.
- Awasthi, S.; Agarwal, D. *Pigm. Resin. Technol.* **2010**, *39*, 208.
- Herrera, M.; Matuschek, G.; Kettrup, A. *Polym. Degrad. Stabil.* **2002**, *78*, 323.

38. Chuang, F. S.; Tsen, W. C.; Shu, Y. C. *Polym. Degrad. Stabil.* **2004**, *84*, 69.
39. Lu, Y. S.; Tighzert, L.; Dole, P.; Erre, D. *Polymer* **2005**, *46*, 9863.
40. Huang, V. T.; Kaletunc, G. *Characterization of Cereals and Flours: Properties, Analysis And Applications*; CRC Press: Boca Raton, **2003**; p 10.
41. Liao, W. H.; Wang, K. W. *J. Sound Vibr.* **1997**, *207*, 319.
42. Sun, W. F.; Zeng, Q. H.; Yu, A. B. *Langmuir* **2013**, *29*, 2175.
43. Sun, W. F.; Zeng, Q. H.; Yu, A. B.; Kendall, K. *Langmuir* **2013**, *29*, 7825.
44. Kim, B. K.; Lee, S. Y.; Xu, M. *Polymer* **1996**, *37*, 5781.
45. Dodiuk, H.; Kariv, O.; Kenig, S.; Tenne, R. *J. Adhes. Sci. Technol.* **2014**, *28*, 38.
46. Cristea, M.; Ibanescu, S.; Cascaval, C. N.; Rosu, D. *High Perform. Polym.* **2009**, *21*, 608.
47. Ni, H.; Daum, J. L.; Thiltgen, P. R.; Soucek, M. D.; Simonsick, W. J.; Zhong, W.; Skaja, A. D. *Prog. Org. Coat.* **2002**, *45*, 49.
48. Sun, W. F. *Nanoscale* **2013**, *5*, 12658.
49. Sun, W. F. *Phys. Chem. Chem. Phys.* **2014**, *16*, 5846.